

1 **Design Principles for High Temperature Superconductors with**  
2 **Hydrogen-based Alloy Backbone at Moderate Pressure**

3 **Zihan Zhang<sup>1</sup>, Tian Cui<sup>2, 1, \*</sup>, Michael J. Hutcheon<sup>3</sup>, Alice M. Shipley<sup>3</sup>, Hao Song<sup>1</sup>, Mingyang**  
4 **Du<sup>1</sup>, Vladimir Z. Kresin<sup>4</sup>, Defang Duan<sup>1, †</sup>, Chris J. Pickard<sup>5, 6</sup>, Yansun Yao<sup>7</sup>**

5  
6 *<sup>1</sup>State Key Laboratory of Superhard Materials, College of Physics, Jilin University, Changchun*  
7 *130012, China*

8 *<sup>2</sup>Institute of High Pressure Physics, School of Physical Science and Technology, Ningbo University,*  
9 *Ningbo, 315211, China*

10 *<sup>3</sup>Theory of Condensed Matter Group, Cavendish Laboratory, University of Cambridge, J. J.*  
11 *Thomson Avenue, Cambridge CB3 0HE, United Kingdom*

12 *<sup>4</sup>Lawrence Berkeley Laboratory, University of California at Berkeley, Berkeley, CA 94720, USA*

13 *<sup>5</sup>Department of Materials Science & Metallurgy, University of Cambridge, 27 Charles Babbage*  
14 *Road, Cambridge CB3 0FS, United Kingdom*

15 *<sup>6</sup>Advanced Institute for Materials Research, Tohoku University 2-1-1 Katahira, Aoba, Sendai, 980-*  
16 *8577, Japan*

17 *<sup>7</sup>Department of Physics and Engineering Physics, University of Saskatchewan, Saskatoon,*  
18 *Saskatchewan, Canada, S7N 5E2*

19  
20  
21  
22  
23  
24 \*Corresponding author. [cuitian@nbu.edu.cn](mailto:cuitian@nbu.edu.cn)

25 †Corresponding author. [duandf@jlu.edu.cn](mailto:duandf@jlu.edu.cn)

26

## Abstract :

Hydrogen-based superconductors provide a route to the long-sought goal of room-temperature superconductivity, but the high pressures required to metallize these materials limit their immediate application. For example, carbonaceous sulfur hydride, the first room-temperature superconductor made in a laboratory, can reach a critical temperature ( $T_c$ ) of 288 K only at the extreme pressure of 267 GPa. The next recognized challenge is the realization of room-temperature superconductivity at significantly lower pressures. Here, we propose a strategy for the rational design of high-temperature superconductors at low pressures by alloying small-radius elements and hydrogen to form ternary H-based superconductors with alloy backbones. We identify a ‘fluorite-type’ backbone in compositions of the form AXH<sub>8</sub>, which exhibit high temperature superconductivity at moderate pressures compared with other reported hydrogen-based superconductors. The  $Fm\bar{3}m$  phase of LaBeH<sub>8</sub>, with a ‘fluorite-type’ H-Be alloy backbone, is predicted to be thermodynamically stable above 98 GPa, and dynamically stable down to 20 GPa with a high  $T_c \sim 185$  K. This is substantially lower than the synthesis pressure required by the geometrically similar clathrate hydride LaH<sub>10</sub> (170 GPa). Our approach paves the way for finding high- $T_c$  ternary H-based superconductors at conditions close to ambient pressures.

1 Hydrogen, the lightest element, has been predicted to become a metallic solid exhibiting high-  
2 temperature superconductivity (with  $T_c$ s in the range 100-760 K) under extreme pressures [1,2].  
3 However, metallization of solid hydrogen is still uncertain in high-pressure experiments up to about  
4 400 GPa [3,4]. It was predicted that comparable high-temperature superconductivity could be achieved  
5 in hydrogen dominant materials by “chemically pre-compressing” the hydrogen with other elements  
6 to produce the valence density sufficient for metallization at lower pressures [5]. Based on this  
7 principle, a series of H-based superconductors were predicted, and some successfully synthesized in  
8 the laboratory. Notably, H<sub>3</sub>S was predicted to be a high-temperature superconductor with a  $T_c$  of 191-  
9 204 K [6], which was later confirmed by an experimentally measured  $T_c$  of 203 K at 155 GPa [7,8].  
10 Following this success, several new hydrides in clathrate hydride family, which consist of a pure  
11 hydrogen backbone pre-compressed by heavy metal atoms, were predicted and then synthesized,  
12 including LaH<sub>10</sub> with a  $T_c$  of 250-260 K at 170-180 GPa [9-12]. Several geometric classes of hydrides  
13 were found to facilitate high  $T_c$ . In addition to the covalent six-fold cubic H<sub>3</sub>S and the sodalite-type  
14 clathrate hydrides, a class of “pentagraphenelike” hydrides with high  $T_c$  were recently predicted at 250  
15 GPa [13]. Although the pressures at which these H-based superconductors become stable (> 150 GPa)  
16 are much lower than the pressure required to metallize pure hydrogen, they are still difficult to obtain.  
17 The next challenge is therefore the realization of room-temperature superconductivity at significantly  
18 lower pressures, with a clear final goal of reaching ambient pressure.

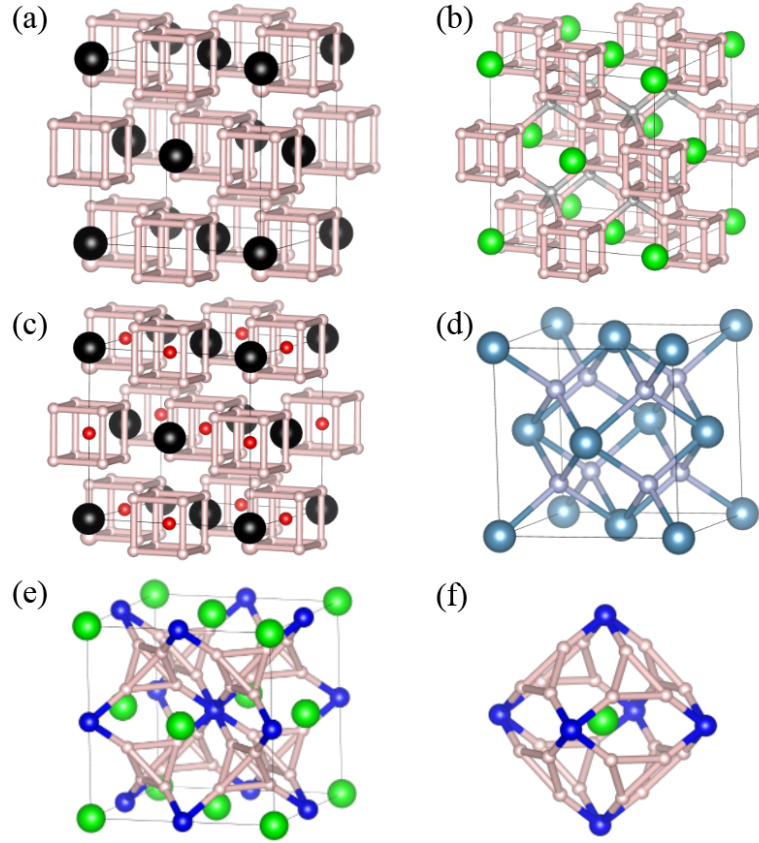
19 Various routes have been explored to reduce the stable pressure of H-based superconductors.  
20 Doping known hydrogen-rich binary systems with dopant elements or molecules is one way to achieve  
21 this. For example, doping a H<sub>3</sub>S host with CH<sub>4</sub> molecules lead to a metastable compound at a much  
22 lower pressure of 100 GPa [14,15]. A careful choice of the elements used for pre-compression is also  
23 important. For example, low-pressure stability in lanthanide and actinide systems correlates strongly  
24 with  $f$  electrons. As a result, metastable phases of YbH<sub>6</sub> and LuH<sub>6</sub> are predicted to have high- $T_c$   
25 superconductivity at relatively low pressures (145 K at 70 GPa and 273 K at 100 GPa, respectively  
26 [16]). Turning to even lower pressures,  $Fm\bar{3}m$  UH<sub>8+ $\delta$</sub>  [17],  $F\bar{4}3m$  EuH<sub>9</sub> [18] and  $C2/c$  NdH<sub>7</sub> [19] have  
27 been observed experimentally at 42 GPa, 86 GPa and 85 GPa, respectively, but the  $T_c$ s in these systems  
28 are very low.

29 Whilst binary hydrides have been extensively explored [20-23], research in ternary hydrides is  
30 more challenging, but rewarding. Many ternary hydrides have been found to exhibit favorable  
31 properties when compared to current binary systems. For example, C doped H<sub>3</sub>S possesses a much  
32 higher  $T_c$  than that of H<sub>3</sub>S in experiments [24], and Li<sub>2</sub>MgH<sub>16</sub>, a molecular Mg-H phase doped with Li,  
33 is predicted to have the highest  $T_c$  to date (473 K) [25]. However, the phase diagrams of ternary systems

1 are much more complex than those of binary systems and therefore require efficient methods to  
2 construct. A recent study shows that a hard-sphere model could help to construct the ternary phase  
3 diagram of hydrides at high pressure [26]. The ability to efficiently explore ternary hydrides and  
4 identify those with desirable superconducting properties at low pressures is key to advancing research  
5 in superconductivity.

6 Here, we propose a strategy to design high- $T_c$  ternary H-based superconductors at low pressures  
7 by engineering binary X-H backbones, which are subsequently “pre-compressed” by a metal element  
8 A. The resulting X-H backbones are easier to metallize than pure H backbones and can be designed by  
9 doping known structures with additional atoms (X), which break the local motif of the parent structure.  
10 This leads to a metallic H-rich phase with occupied overlapping bands, known as a *hydrogen alloy*  
11 phase [5]. We first designed a novel class of fluorite-type ternary structures  $AXH_8$  ( $Fm\bar{3}m$ ), from  
12 which we found 7 dynamically stable H-based superconductors consisting of a “pre-compressor”  
13 element A (A = Sc, Ca, Y, Sr, La, Ba) and a small-radius element X (X = Be, B, Al). This is followed  
14 by the construction of a hard-sphere model to investigate new fluorite-type hydrides and the stability  
15 of these new materials in terms of geometrical factors.

16 We design the first of these alloy backbone materials from the pure H backbone of the high-  
17 temperature superconductor  $LaH_{10}$  [12], which possesses the same symmetry as the low-pressure  $UH_8$   
18 superconductor [17]. Comparing the crystal structures of  $UH_8$  and  $LaH_{10}$  (Fig. 1(a)-(b)), the structure  
19 of  $LaH_{10}$  can be viewed as a  $UH_8$  parent structure doped with additional H atoms at vacant tetrahedral  
20 sites. The extra H atoms break the localization of cubic  $H_8$  units and lead to the famous clathrate  
21 backbone in  $LaH_{10}$ . Instead, dopant X atoms can be inserted in vacancy sites at the centre of the cubic  
22  $H_8$  units, resulting in an  $Fm\bar{3}m$  structure of  $LaXH_8$  (Fig. 1(c)). For example, Be may be a suitable  
23 dopant at these cubic sites. This novel H-Be alloy backbone corresponds to a fluorite-type arrangement  
24 (Fig. 1(d)), in which Be atoms are located on the sites of a face-centered cubic lattice, and  $[H_4]$   
25 tetrahedra are present in the tetrahedral vacancies found between the Be atoms (Figs. 1(e)-(f)). Ternary  
26 hydrides  $AXH_8$ , designed with X-H alloy backbones, potentially achieve high-temperature  
27 superconductivity at lower predicted pressures than the required pressures of other reported H-based  
28 superconductors. We note that during the preparation of our manuscript, the same cubic structure was  
29 reported in the La-B-H ternary system by two different groups [27-29].

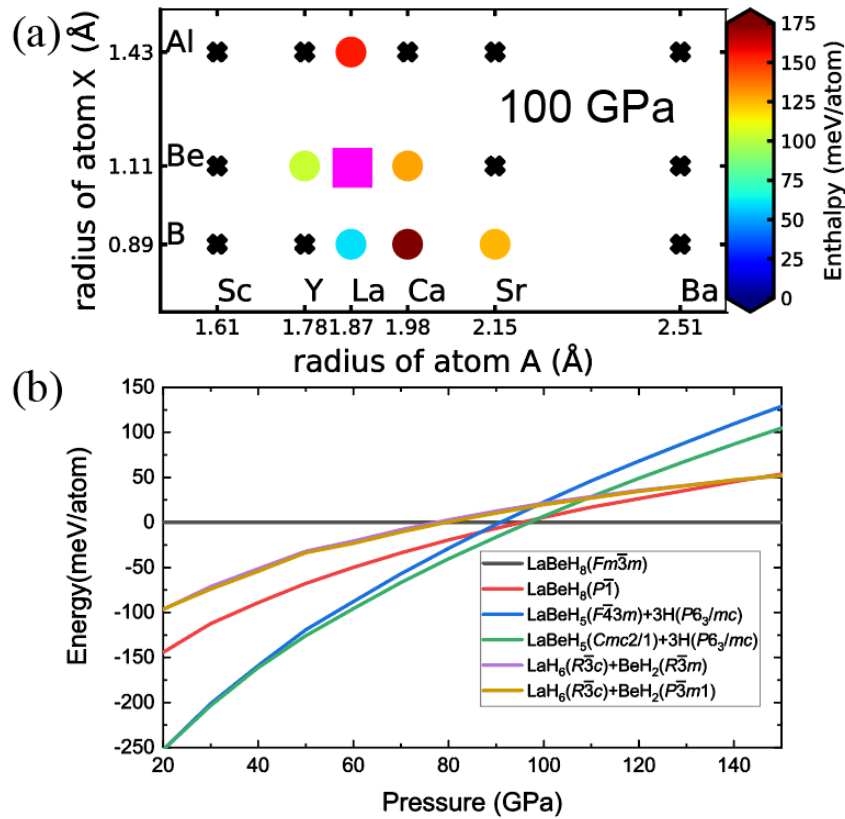


1

2 FIG. 1 (a) The crystal structure of  $\text{UH}_8$  with  $[\text{H}_8]$  cubic units. The U ions are shown in black  
 3 and the H ions in pink. (b) The crystal structure of  $\text{LaH}_{10}$ , in which La ions are shown in green.  
 4 The backbone in  $\text{LaH}_{10}$  consists of cubic-unit H atoms (pink) and tetrahedron-center H atoms  
 5 (gray). (c) The crystal structure of  $\text{UH}_8$ , with  $[\text{H}_8]$  cubic centers shown as red balls. (d) The  
 6 crystal structure of fluorite  $\text{CaF}_2$ , the Ca cations are shown in dark blue and the F ions in light  
 7 blue. (e) The crystal structure of  $\text{LaBeH}_8$ . The backbone in  $\text{LaBeH}_8$  consists of tetrahedral-  
 8 unit H atoms (pink) and cubic-center Be atoms (blue). (f) The ‘fluorite-type’ cage of  $\text{LaBeH}_8$ .

9 Having identified this fluorite-type ternary structure, we go on to investigate the wider class of  
 10 fluorite-type backbone hydrides  $\text{AXH}_8$  ( $Fm\bar{3}m$ ), consisting of a ‘‘pre-compressor’’ element A (A = Sc,  
 11 Ca, Y, Sr, La, Ba) and a small-radius element X (X = Be, B, Al). Among the resulting 18 combinations  
 12 for  $\text{AXH}_8$  ternary hydrides, 7 exhibit regions of dynamic stability within the range of pressures studied  
 13 in this work, as established by the absence of imaginary frequencies in phonon dispersions (Figs. S1-  
 14 S8 of SM [30]). These hydrides are  $\text{LaBeH}_8$ ,  $\text{CaBeH}_8$ ,  $\text{YBeH}_8$ ,  $\text{CaBH}_8$ ,  $\text{SrBH}_8$ ,  $\text{LaBH}_8$  and  $\text{LaAlH}_8$ .  
 15 Notably,  $\text{LaBeH}_8$  remains dynamically stable at pressures as low as 20 GPa. The other 11 hydrides are  
 16 unstable within the studied pressure range, exhibiting imaginary phonon modes that break crystal  
 17 symmetry (Figs. S12-S22 of SM [30]). Having identified 7 dynamically stable ‘‘fluorite-type’’ hydrides,  
 18 we go on to determine their thermodynamic stability using *ab initio* random structure searching  
 19 (AIRSS) [31], by constructing convex hulls (Fig. S24-S30 of SM [30]). Combining the phonon

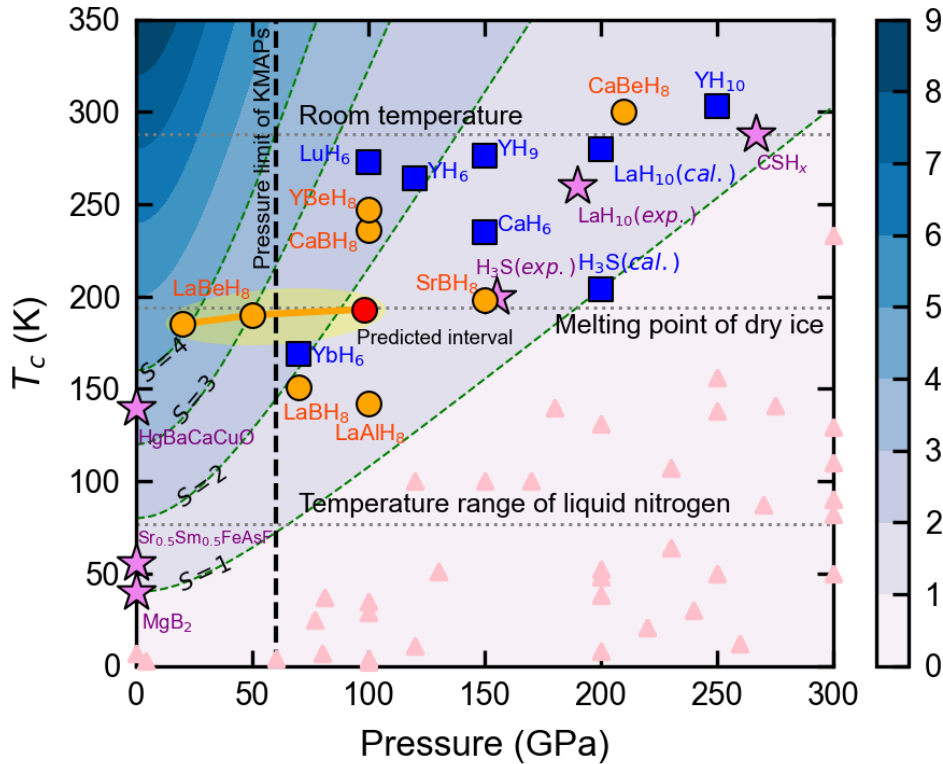
1 dispersion analysis (Fig. S1 of SM [30]) with enthalpy difference calculations (Fig. 2b), we find that  
 2 cubic  $\text{LaBeH}_8$  becomes thermodynamically stable above 98 GPa. However, its dynamical stability  
 3 (metastability) may be retained as low as 20 GPa.  $\text{YBeH}_8$  and  $\text{SrBH}_8$  become thermodynamically  
 4 stable at 300 GPa (Fig. S23 of SM [30]). The other four hydrides that exhibit dynamical stability,  
 5  $\text{CaBeH}_8$ ,  $\text{CaBH}_8$ ,  $\text{LaBH}_8$  and  $\text{LaAlH}_8$ , are not thermodynamically stable within the studied pressure  
 6 range ( $\leq 300$  GPa), but are likely to become so at much high pressures. According to the Inorganic  
 7 Crystal Structure Database, 20% of synthesized materials are metastable, some of which even have  
 8 positive formation enthalpies. High-pressure synthesis usually involves high temperatures, and  
 9 therefore the products are often metastable; synthesized diamond and nitrogen allotropes are good  
 10 examples. The experimentally discovered superconducting systems Si-H [51] and S-C-H [24] are also  
 11 found to be metastable in theoretical calculations. Anharmonicity was found to play an important role  
 12 in some superconducting hydrides [52,53]. However, current calculations do not allow a high-  
 13 throughput evaluation of anharmonic effects in structure prediction.



14  
 15 FIG. 2 Calculated enthalpy of “fluorite-type” hydrides  $\text{AXH}_8$ . (a) The radius of atom A is plotted  
 16 on the x-axis and the radius of atom X on the y-axis. Dynamically unstable systems are shown  
 17 as black crosses. Metastable phases are shown as circles, colored according to the  
 18 calculated enthalpy above the convex hull. Thermodynamically stable phases are shown as  
 19 carmine squares. (b) Calculated enthalpy as a function of pressure for La-Be-H structures

1 relative to the  $Fm\bar{3}m$  phase of  $\text{LaBeH}_8$ , where structures of  $\text{LaH}_6$ ,  $\text{BeH}_2$  and H are from Refs.  
 2 [9-11,39,54], respectively.

3 Having investigated the stability of these fluorite-type backbone hydrides, we go on to investigate  
 4 their superconducting properties. From the Eliashberg equations in Sec. 3 of SM [30], the values of  $T_c$   
 5 were determined using  $\mu^* = 0.1$ . As shown in Fig. 3,  $\text{LaBeH}_8$  is predicted to exhibit high-temperature  
 6 superconductivity with a  $T_c$  of 192 K at 100 GPa and 183 K at 20 GPa (threshold for metastability).  
 7 The  $T_c$  values calculated using the McMillan equation and Gorkov-Kresin theory are presented and  
 8 discussed in the SM [30]. These fluorite-type backbone structures also have the potential to exhibit  
 9 room-temperature superconductivity, with the metastable  $\text{CaBeH}_8$  predicted to possess a  $T_c$  of 300 K  
 10 at 210 GPa. Likewise, we calculate that  $\text{YBeH}_8$ ,  $\text{CaBH}_8$ ,  $\text{SrBH}_8$ ,  $\text{LaBH}_8$  and  $\text{LaAlH}_8$  exhibit high  
 11 temperature superconductivity within their metastable region, with  $T_c$ s of 249 K at 100 GPa, 238 K at  
 12 100 GPa, 200 K at 150 GPa, 160 K at 70 GPa and 144 K at 100 GPa, respectively. A common feature  
 13 of these superconducting hydrides is the occurrence of soft phonon modes at the Brillouin zone  
 14 boundary (Figs. S1-S8 in SM [30]), leading to strong electron-phonon coupling. This effect is stronger  
 15 when the system is close to instability. As shown in Fig. 3, the threshold pressure at which fluorite-  
 16 type backbone hydrides become dynamically stable is lower than that for typical high- $T_c$  hydrides,  
 17 whilst retaining a  $T_c$  that is much higher than the temperature of liquid nitrogen.  $\text{LaBeH}_8$  is the first  
 18 proposed H-based superconductor with a figure of merit [55] score around  $S = 3\sim 4$ .



1 FIG. 3 Pressure dependence of  $T_c$ s for typical superconductors. The orange circles are  $T_c$ s  
 2 of fluorite-type backbone hydrides at the lowest pressure where they become dynamically  
 3 stable. The red circle is at the lowest pressure where LaBeH<sub>8</sub> becomes thermodynamically  
 4 stable (98 GPa), and the suggested synthesis pressure range for cubic LaBeH<sub>8</sub> is highlighted  
 5 in yellow. The blue squares are  $T_c$ s of clathrate binary hydrides at the lowest pressures  
 6 reported in Refs. [6,9,10,40,55]. The purple stars are  $T_c$ s of well-known superconductors from  
 7 experiment [7,12,24,55]. The background is shaded according to the figure of merit  $S =$   
 8  $\frac{T}{\sqrt{P^2 + T_{MgB_2}^2}}$  used to evaluate the significance of a particular superconductor [55]. The dotted  
 9 line is the pressure limit of Kawai-type multi-anvil presses (KMAPs) [56].

10 Geometrical factors play an important role in the high-throughput screening of materials such as  
 11 perovskites [57] and MXenes [58]. Effective hard-sphere models can be used as structural prototypes  
 12 in the exploration of such novel materials [26]. The dynamic stability of fluorite-type hydrides depends  
 13 on the radii of the pre-compressor element A, suggesting that a hard-sphere model [59] derived from  
 14 geometrical factors may allow us to draw general conclusions about this family of structures. To  
 15 construct this model, we make two simplifications: i) the “pre-compressors” A are regarded as hard  
 16 spheres; ii) the backbone is characterized by H-H bonds and X-H bonds. The derivation of this model  
 17 is presented in Sec. 5 of SM [30] and the solution gives the lattice parameter of the cubic unit cell ( $L$ ),  
 18 the lengths of H-H bonds ( $b_{H-H}$ ) and X-H bonds ( $b_{X-H}$ ) as follows:

$$19 \left\{ \begin{array}{l} L = \frac{\sqrt{3}+1}{t+1} \cdot 2R_A \\ b_{H-H} = \frac{\sqrt{3}+1-2t}{t+1} \cdot \sqrt{6}R_A = F_{H-H}d_{H-H}, \\ b_{X-H} = \frac{3t-\sqrt{3}}{t+1} \cdot R_A = F_{H-X}d_{H-X} \end{array} \right.$$

20 where  $R_A$  is the covalent radius [50] of atom A and  $t = 0.95-1.05$  is a tolerance factor allowing  
 21 slight overlap of the hard spheres. The bond lengths can also be represented as products of flexible  
 22 factors ( $F$ ) and bond lengths of binary hydrides ( $d$ ) from the literatures.

23 The solved  $L$ ,  $b_{H-H}$  and  $b_{X-H}$  for the 7 hydrides using the hard sphere model are shown in Table 1,  
 24 alongside with the values calculated from DFT at 150 GPa. The value of  $L$  obtained in the hard spheres  
 25 model is similar to that calculated by DFT in the pressure range of 100-200 GPa. The geometry of the  
 26 fluorite-type backbone has elongated the H-H bond lengths by 30-60% or 20-30% (according to the  
 27 hard-spheres model and DFT, respectively) compared to the H-H bond lengths in common hydrides  
 28 [9,13,25], because of the large amount of charge transferred to the H-H bond (Table 1). The X-H bonds  
 29 are also affected by the geometry, but whether the bonds are elongated or shortened depends on the



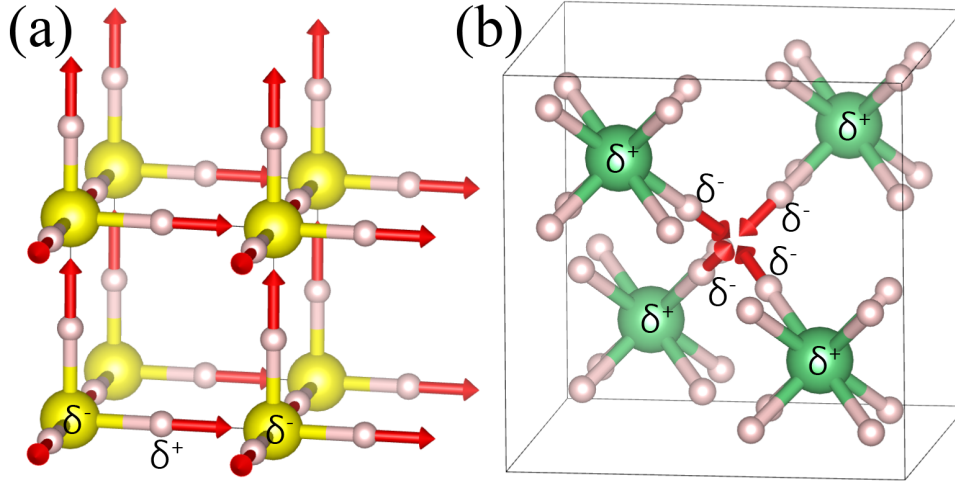
1 composition; with the hard-spheres model and DFT calculations in agreement. Clearly, geometric  
 2 factors are crucial to understanding the stability of “fluorite-type” hydrides.

3

4 Table. 1 The lattice parameter  $L$ , bond lengths  $b_{X-H}$  and  $b_{H-H}$  and flexible factors  $F$  calculated  
 5 from the hard-spheres model (unprimed) and from DFT (primed) at 150 GPa. The amount of  
 6 charge transferred to H is denoted as  $\delta$ . Here we use  $t=1.03$ ,  $d_{H-H}=1.1$  Å [9,13,25],  $d_{Be-H} =$   
 7  $1.31$  Å [39],  $d_{B-H} = 1.22$  Å [42] and  $d_{Al-H} = 1.72$  Å [44,60].

	$L, \text{Å}$	$b_{X-H}, \text{Å}$ ( $F_{X-H}$ )	$b_{H-H}, \text{Å}$ ( $F_{H-H}$ )	$L', \text{Å}$	$b'_{X-H}, \text{Å}$ ( $F'_{X-H}$ )	$b'_{H-H}, \text{Å}$ ( $F'_{H-H}$ )	$\delta, e^-/\text{atom}$
LaBeH <sub>8</sub>	5.03	1.25 (91%)	1.52 (137%)	5.17	1.36 (99%)	1.43 (130%)	0.36
LaBH <sub>8</sub>	5.03	1.25 (102%)	1.52 (137%)	5.13	1.33 (109%)	1.45 (131%)	0.32
LaAlH <sub>8</sub>	5.03	1.25 (73%)	1.52 (137%)	5.38	1.52 (88%)	1.32 (120%)	0.46
SrBH <sub>8</sub>	5.79	1.44 (118%)	1.74 (158%)	5.05	1.32 (108%)	1.41 (128%)	0.29
CaBH <sub>8</sub>	5.33	1.32 (109%)	1.60 (146%)	4.89	1.3 (107%)	1.33 (121%)	0.29
CaBeH <sub>8</sub>	5.33	1.32 (97%)	1.60 (146%)	4.93	1.32 (96%)	1.32 (120%)	0.32
YBeH <sub>8</sub>	4.79	1.19 (86%)	1.44 (131%)	5.02	1.34 (98%)	1.36 (124%)	0.40

8 The hard-spheres model captures the general characteristics of AXH<sub>8</sub> and allows us to determine  
 9 the criteria for elements that can be substituted for X in the crystal. In particular, candidate elements  
 10 should form bonds to hydrogen with lengths in the range of 1.2-1.6 Å in binary systems. Therefore,  
 11 we investigate the possibility of substituting Si, P and S into LaXH<sub>8</sub> since the X-H bond lengths are  
 12  $d_{Si-H} \sim 1.6$  Å [61],  $d_{P-H} \sim 1.4$  Å [62] and  $d_{S-H} \sim 1.5$  Å [63]. We find that LaSiH<sub>8</sub>, LaSH<sub>8</sub> and LaPH<sub>8</sub> are  
 13 all dynamically stable below 200 GPa (Fig. S9-11 of SM [30]), and they are calculated to exhibit high-  
 14  $T_c$  superconductivity: 150 K at 100 GPa, 195 K at 200 GPa and 151 K at 200 GPa (Fig. S50-52),  
 15 respectively.



1

2 FIG. 4 (a) The polarization vectors of H-S bonds in [H<sub>3</sub>S] backbone; in these bonds the  
 3 positive charge is located at H atoms (pink) and negative charge is located at S atoms  
 4 (yellow). (b) The polarization vectors of Be-H bonds in [BeH<sub>3</sub>] backbone converge, leading to  
 5 a concentration of charge at the hydrogen atoms. In these bonds the positive charge is  
 6 located at Be atoms (green) and the negative charge is located at H atoms (pink).

7

8 Binary backbones in hydrides typically consist of polar bonds at high pressure. For example, the  
 9 [SH<sub>3</sub>] backbone of SCH<sub>7</sub> consists of H-S polar bonds (see Fig. 4(a)). End-to-end arrangements of polar  
 10 bonds in these backbones generally have low enthalpy. But in the [BeH<sub>8</sub>] backbone four H atoms with  
 11 negative charge δ<sup>-</sup> are found in close proximity (see Fig. 4(b)), suggesting that the fluorite-type  
 12 backbone is formed in a different way. In the unique bonding environment of the fluorite-type  
 13 backbone, a large amount of charge transfer to the H atoms is possible as shown in Table 1; these  
 14 electrons occupy anti-bonding states along the H-H bonds (Fig.S56-S62 of SM [30]). These extra  
 15 electrons not only support the elongated H-H bonds, but also give rise to an increased H-derived  
 16 density of states at the Fermi level. The unique chemistry in alloyed backbones therefore provides a  
 route to improved H-based superconductors.

17

18 As part of efforts toward developing H-based superconductors that are stable at low pressure, we  
 19 design a class of ternary hydrides AXH<sub>8</sub> with fluorite-type alloy backbones. Compared with other  
 20 reported H-based superconductors, the predicted AXH<sub>8</sub> hydrides exhibit dynamic stability at pressures  
 21 much lower than their thermodynamic region, whilst maintaining the strong electron-phonon coupling  
 22 necessary for high T<sub>c</sub> superconductivity. One of the systems we considered, LaBeH<sub>8</sub>, is dynamically  
 23 stable down to 20 GPa which is much lower than both the pressure needed to stabilize typical H-based  
 24 superconductors and the pressure obtainable in KMAPs. The hydrides in the fluorite-type backbone  
 25 family would have about 20 members if other elements in the lanthanide and actinide series were  
 included. Future investigations of other ternary systems may identify high-temperature

1 superconductors even closer to ambient pressure by similar methods.

2         In summary, designing hydrides with an alloyed backbone is shown to be an effective approach  
3 to obtaining low-pressure H-based superconductors. In these materials, small radius elements are  
4 alloyed with hydrogen to introduce new bonds into the backbone structure, replacing some H-H bonds.  
5 Our results will stimulate further experimental exploration and the synthesis of hydride-based  
6 superconductors at near ambient pressures would represent an important breakthrough in the field of  
7 high-temperature superconductivity.

## 8 **Acknowledgements**

9 This work was supported by the National Natural Science Foundation of China (Grants No. 12122405,  
10 No. 11974133, No. 51632002, No. 11674122), National Key R&D Program of China (Grant No.  
11 2018YFA0305900), Program for Changjiang Scholars and Innovative Research Team in University  
12 (Grant No. IRT\_15R23), and the Natural Sciences and Engineering Research Council of Canada  
13 (NSERC). C.J.P. acknowledges financial support from the Engineering and Physical Sciences  
14 Research Council (Grant EP/P022596/1) and a Royal Society Wolfson Research Merit award. AMS is  
15 funded by an EPSRC studentship. MJH acknowledges the EPSRC Centre for Doctoral Training in  
16 Computational Methods for Materials Science for funding under grant number EP/L015552/1. Some  
17 of the calculations were performed at the High Performance Computing Center of Jilin University and  
18 using TianHe-1(A) at the National Supercomputer Center in Tianjin.

19

20

- 1 [1] E. Wigner and H. B. Huntington, *On the Possibility of a Metallic Modification of Hydrogen*, J. Chem. Phys. 2 **3**, 764, (1935).
- 3 [2] J. M. McMahon, M. A. Morales, C. Pierleoni, and D. M. Ceperley, *The properties of hydrogen and helium* 4 *under extreme conditions*, Rev. Mod. Phys. **84**, 1607, (2012).
- 5 [3] P. Dalladay-Simpson, R. T. Howie, and E. Gregoryanz, *Evidence for a new phase of dense hydrogen above* 6 *325 gigapascals*, Nature **529**, 63, (2016).
- 7 [4] P. Loubeyre, F. Occelli, and P. Dumas, *Synchrotron infrared spectroscopic evidence of the probable* 8 *transition to metal hydrogen*, Nature **577**, 631, (2020).
- 9 [5] N. W. Ashcroft, *Hydrogen dominant metallic alloys: High temperature superconductors?*, Phys. Rev. Lett. 10 **92**, 187002, (2004).
- 11 [6] D. Duan, Y. Liu, F. Tian, D. Li, X. Huang, Z. Zhao, H. Yu, B. Liu, W. Tian, and T. Cui, *Pressure-induced* 12 *metallization of dense  $(H_2S)_2H_2$  with high- $T_c$  superconductivity*, Sci. Rep. **4**, 6968, (2014).
- 13 [7] A. P. Drozdov, M. I. Eremets, I. A. Troyan, V. Ksenofontov, and S. I. Shylin, *Conventional superconductivity* 14 *at 203 kelvin at high pressures in the sulfur hydride system*, Nature **525**, 73, (2015).
- 15 [8] M. Einaga, M. Sakata, T. Ishikawa, K. Shimizu, M. I. Eremets, A. P. Drozdov, I. A. Troyan, N. Hirao, and Y. 16 Ohishi, *Crystal structure of the superconducting phase of sulfur hydride*, Nature Phys. **12**, 835, (2016).
- 17 [9] H. Liu, I. I. Naumov, R. Hoffmann, N. W. Ashcroft, and R. J. Hemley, *Potential high- $T_c$  superconducting* 18 *lanthanum and yttrium hydrides at high pressure*, Proc. Natl. Acad. Sci. U. S. A. **114**, 6990, (2017).
- 19 [10] F. Peng, Y. Sun, C. J. Pickard, R. J. Needs, Q. Wu, and Y. M. Ma, *Hydrogen Clathrate Structures in Rare Earth* 20 *Hydrides at High Pressures: Possible Route to Room-Temperature Superconductivity*, Phys. Rev. Lett. **119**, 107001, 21 (2017).
- 22 [11] A. M. Shipley, M. J. Hutcheon, M. S. Johnson, R. J. Needs, and C. J. Pickard, *Stability and superconductivity* 23 *of lanthanum and yttrium decahydrides*, Phys. Rev. B **101**, 224511, (2020).
- 24 [12] A. P. Drozdov, P. P. Kong, V. S. Minkov, S. P. Besedin, M. A. Kuzovnikov, S. Mozaffari, L. Balicas, F. F. Balakirev, 25 D. E. Graf, V. B. Prakapenka, E. Greenberg, D. A. Knyazev, M. Tkacz, and M. I. Eremets, *Superconductivity at 250 K* 26 *in lanthanum hydride under high pressures*, Nature **569**, 528, (2019).
- 27 [13] H. Xie, Y. Yao, X. Feng, D. Duan, H. Song, Z. Zhang, S. Jiang, S. A. T. Redfern, V. Z. Kresin, C. J. Pickard, and 28 T. Cui, *Hydrogen Pentagraphenelike Structure Stabilized by Hafnium: A High-Temperature Conventional* 29 *Superconductor*, Phys. Rev. Lett. **125**, 217001 (2020).
- 30 [14] Y. Sun, Y. Tian, B. Jiang, X. Li, H. Li, T. litaka, X. Zhong, and Y. Xie, *Computational discovery of a dynamically* 31 *stable cubic SH3-like high-temperature superconductor at 100 GPa via CH4 intercalation*, Phys. Rev. B **101**, 174102 32 (2020).
- 33 [15] W. Cui, T. Bi, J. Shi, Y. Li, H. Liu, E. Zurek, and R. J. Hemley, *Route to high- $T_c$  superconductivity via CH4-* 34 *intercalated H3S hydride perovskites*, Phys. Rev. B **101**, 134504 (2020).
- 35 [16] Hao Song, Zihan Zhang, Tian Cui, V. Chris J. Pickard, Iadimir Z. Kresin, and D. Duan, *High  $T_c$*  36 *Superconductivity in Heavy Rare Earth Hydrides*, Chin. Phys. Lett., 107401%V 38, (2021).
- 37 [17] I. A. Kruglov, A. G. Kvashnin, A. F. Goncharov, A. R. Oganov, S. S. Lobanov, N. Holtgrewe, S. Jiang, V. B. 38 Prakapenka, E. Greenberg, and A. V. Yanilkin, *Uranium polyhydrides at moderate pressures: Prediction, synthesis,* 39 *and expected superconductivity*, Sci. Adv. **4**, 7, (2018).
- 40 [18] D. V. Semenov, D. Zhou, A. G. Kvashnin, X. Huang, M. Galasso, I. A. Kruglov, A. G. Ivanova, A. G. Gavriliuk, 41 W. Chen, N. V. Tkachenko, A. I. Boldyrev, I. Troyan, A. R. Oganov, and T. Cui, *Novel Strongly Correlated Europium* 42 *Superhydrides*, J. Phys. Chem. Lett. **12**, 32, (2021).
- 43 [19] D. Zhou, D. V. Semenov, H. Xie, X. L. Huang, D. F. Duan, A. Aperis, P. M. Oppeneer, M. Galasso, A. I. Kartsev, 44 A. G. Kvashnin, A. R. Oganov, and T. Cui, *High-Pressure Synthesis of Magnetic Neodymium Polyhydrides*, J. Am. 45 Chem. Soc. **142**, 2803, (2020).
- 46 [20] D. F. Duan, Y. X. Liu, Y. B. Ma, Z. Shao, B. B. Liu, and T. Cui, *Structure and superconductivity of hydrides at* 47 *high pressures*, Natl. Sci. Rev. **4**, 121, (2017).
- 48 [21] A. R. Oganov, C. J. Pickard, Q. Zhu, and R. J. Needs, *Structure prediction drives materials discovery*, Nat. 49 Rev. Mater. **4**, 331, (2019).
- 50 [22] E. Zurek and T. G. Bi, *High-temperature superconductivity in alkaline and rare earth polyhydrides at high* 51 *pressure: A theoretical perspective*, J. Chem. Phys. **150**, 13, (2019).

- 1 [23] J. A. Flores-Livas, L. Boeri, A. Sanna, G. Profeta, R. Arita, and M. Eremets, *A perspective on conventional*  
2 *high-temperature superconductors at high pressure: Methods and materials*, Phys. Rep. **856**, 1, (2020).
- 3 [24] E. Snider, N. Dasenbrock-Gammon, R. McBride, M. Debessai, H. Vindana, K. Vencatasamy, K. V. Lawler, A.  
4 Salamat, and R. P. Dias, *Room-temperature superconductivity in a carbonaceous sulfur hydride*, Nature **586**, 373,  
5 (2020).
- 6 [25] Y. Sun, J. Lv, Y. Xie, H. Liu, and Y. Ma, *Route to a Superconducting Phase above Room Temperature in*  
7 *Electron-Doped Hydride Compounds under High Pressure*, Phys. Rev. Lett. **123**, 097001 (2019).
- 8 [26] R. Koshiji and T. Ozaki, *Densest ternary sphere packings*, Phys. Rev. E **104**, 024101, (2021).
- 9 [27] S. Di Cataldo, W. von der Linden, and L. Boeri, *La-X-H hydrides: is hot superconductivity possible?*, arXiv  
10 e-prints, arXiv:2106.07266, (2021).
- 11 [28] S. Di Cataldo, C. Heil, W. von der Linden, and L. Boeri, *LaBH8: Towards high-Tc low-pressure*  
12 *superconductivity in ternary superhydrides*, Phys. Rev. B **104**, L020511, (2021).
- 13 [29] X. Liang, A. Bergara, X. Wei, L. Wang, and Y. Tian, *Prediction of high-Tc superconductivity in ternary*  
14 *lanthanum borohydrides*, arXiv e-prints, arXiv:2107.02553, (2021).
- 15 [30] *See Supplemental Material for computational details, phonon band structure of "fluorite-type" hydrides,*  
16 *the ternary convex hull of "fluorite-type" backbone hydrides, equations for calculating Tc and related parameters,*  
17 *the hard-sphere model of "fluorite-type" backbone hydride, the Crystalline Orbital Hamiltonian Population*  
18 *(COHP) and Integrated Crystalline Orbital Hamiltonian Population (ICOHP) of "fluorite-type" backbone hydride,*  
19 *electronic structure of "fluorite-type" backbone hydrides and structural information.,* (Includes Refs. [9,28,29,31-  
20 50]).
- 21 [31] C. J. Pickard and Needs, *Ab initio random structure searching*, J. Phys.-Condes. Matter **23**, 053201 (2011).
- 22 [32] M. D. Segall, P. J. D. Lindan, M. J. Probert, C. J. Pickard, P. J. Hasnip, S. J. Clark, and M. C. Payne, *First-*  
23 *principles simulation: ideas, illustrations and the CASTEP code*, J. Phys.-Condes. Matter **14**, 2717, (2002).
- 24 [33] G. Kresse and J. Furthmüller, *Efficiency of ab-initio total energy calculations for metals and semiconductors*  
25 *using a plane-wave basis set*, Comput. Mater. Sci. **6**, 15, (1996).
- 26 [34] J. P. Perdew, K. Burke, and Y. Wang, *Generalized gradient approximation for the exchange-correlation hole*  
27 *of a many-electron system*, Phys. Rev. B **54**, 16533, (1996).
- 28 [35] W. Tang, E. Sanville, and G. Henkelman, *A grid-based Bader analysis algorithm without lattice bias*, J. Phys.-  
29 Condes. Matter **21**, 084204, (2009).
- 30 [36] V. L. Deringer, A. L. Tchougréeff, and R. Dronskowski, *Crystal Orbital Hamilton Population (COHP) Analysis*  
31 *As Projected from Plane-Wave Basis Sets*, J. Phys. Chem. A **115**, 5461, (2011).
- 32 [37] P. Giannozzi, S. Baroni, N. Bonini, M. Calandra, R. Car, C. Cavazzoni, D. Ceresoli, G. L. Chiarotti, M.  
33 Cococcioni, I. Dabo, A. Dal Corso, S. De Gironcoli, S. Fabris, G. Fratesi, R. Gebauer, U. Gerstmann, C. Gougoussis, A.  
34 Kokalj, M. Lazzeri, L. Martin-Samos, N. Marzari, F. Mauri, R. Mazzarello, S. Paolini, A. Pasquarello, L. Paulatto, C.  
35 Sbraccia, S. Scandolo, G. Sclauzero, A. P. Seitsonen, A. Smogunov, P. Umari, and R. M. Wentzcovitch, *QUANTUM*  
36 *ESPRESSO: A modular and open-source software project for quantum simulations of materials*, J. Phys.-Condes.  
37 Matter **21**, 395502, (2009).
- 38 [38] G. Kresse and D. Joubert, *From ultrasoft pseudopotentials to the projector augmented-wave method*, Phys.  
39 Rev. B **59**, 1758, (1999).
- 40 [39] Z. Wang, Y. Yao, L. Zhu, H. Liu, T. litaka, H. Wang, and Y. Ma, *Metallization and superconductivity of BeH<sub>2</sub>*  
41 *under high pressure*, J. Chem. Phys. **140**, 124707, (2014).
- 42 [40] H. Wang, S. T. John, K. Tanaka, T. litaka, and Y. Ma, *Superconductive sodalite-like clathrate calcium hydride*  
43 *at high pressures*, Proc. Natl. Acad. Sci. U. S. A. **109**, 6463, (2012).
- 44 [41] Z. Shao, D. Duan, Y. Ma, H. Yu, H. Song, H. Xie, D. Li, F. Tian, B. Liu, and T. Cui, *Unique Phase Diagram and*  
45 *Superconductivity of Calcium Hydrides at High Pressures*, Inorg. Chem. **58**, 2558, (2019).
- 46 [42] C. H. Hu, A. R. Oganov, Q. Zhu, G. R. Qian, G. Frapper, A. O. Lyakhov, and H. Y. Zhou, *Pressure-induced*  
47 *stabilization and insulator-superconductor transition of BH*, Phys. Rev. Lett. **110**, 165504, (2013).
- 48 [43] Y. Wang, H. Wang, J. S. Tse, T. litaka, and Y. Ma, *Structural morphologies of high-pressure polymorphs of*  
49 *strontium hydrides*, Phys. Chem. Chem. Phys. **17**, 19379, (2015).
- 50 [44] I. Goncharenko, M. I. Eremets, M. Hanfland, J. S. Tse, M. Amboage, Y. Yao, and I. A. Trojan, *Pressure-induced*  
51 *hydrogen-dominant metallic state in aluminum hydride*, Phys. Rev. Lett. **100**, 045504, (2008).

- 1 [45] G. M. Eliashberg, *Interactions between electrons and lattice vibrations in a superconductor*, Sov. Phys. **11**,  
2 696, (1960).
- 3 [46] L. P. Gor'kov and V. Z. Kresin, *Colloquium: High pressure and road to room temperature superconductivity*,  
4 Rev. Mod. Phys. **90**, 011001 (2018).
- 5 [47] P. B. Allen and R. C. Dynes, *Transition temperature of strong-coupled superconductors reanalyzed*, Phys.  
6 Rev. B **12**, 905, (1975).
- 7 [48] S. Poncé, E. R. Margine, C. Verdi, and F. Giustino, *EPW: Electron-phonon coupling, transport and*  
8 *superconducting properties using maximally localized Wannier functions*, Comput. Phys. Commun. **209**, 116, (2016).
- 9 [49] M. Wierzbowska, S. D. Gironcoli, and P. Giannozzi, *Origins of low- and high-pressure discontinuities of  $T_c$*   
10 *in niobium*, arXiv e-prints, arXiv:cond, (2005).
- 11 [50] R. Heyrovska, *Atomic, Ionic and Bohr Radii Linked via the Golden Ratio for Elements of Groups 1 - 8*  
12 *Including Lanthanides and Actinides*, Inter. J. Sci. **2**, 63, (2013).
- 13 [51] I. A. T. M. I. Eremets, S. A. Medvedev, J. S. Tse, Y. Yao, *Superconductivity in Hydrogen Dominant Materials*  
14 *Silane*, Science **319**, 1506, (2008).
- 15 [52] I. Errea, M. Calandra, C. J. Pickard, J. R. Nelson, R. J. Needs, Y. W. Li, H. Y. Liu, Y. W. Zhang, Y. M. Ma, and F.  
16 Mauri, *Quantum hydrogen-bond symmetrization in the superconducting hydrogen sulfide system*, Nature **532**, 81,  
17 (2016).
- 18 [53] I. Errea, F. Belli, L. Monacelli, A. Sanna, T. Koretsune, T. Tadano, R. Bianco, M. Calandra, R. Arita, F. Mauri,  
19 and J. A. Flores-Livas, *Quantum crystal structure in the 250-kelvin superconducting lanthanum hydride*, Nature **578**,  
20 66, (2020).
- 21 [54] C. J. Pickard and R. J. Needs, *Structure of phase III of solid hydrogen*, Nature Phys. **3**, 473, (2007).
- 22 [55] C. J. Pickard, I. Errea, and M. I. Eremets, *Superconducting Hydrides Under Pressure*, Annu. Rev. Condens.  
23 Matter Phys. **11**, 57, (2020).
- 24 [56] T. Ishii, Z. D. Liu, and T. Katsura, *A Breakthrough in Pressure Generation by a Kawai-Type Multi-Anvil*  
25 *Apparatus with Tungsten Carbide Anvils*, Engineering **5**, 434, (2019).
- 26 [57] S. Lu, Q. Zhou, Y. Ouyang, Y. Guo, Q. Li, and J. Wang, *Accelerated discovery of stable lead-free hybrid*  
27 *organic-inorganic perovskites via machine learning*, Nat. Commun. **9**, 3405 (2018).
- 28 [58] N. C. Frey, J. Wang, G. I. Vega Bellido, B. Anasori, Y. Gogotsi, and V. B. Shenoy, *Prediction of Synthesis of*  
29 *2D Metal Carbides and Nitrides (MXenes) and Their Precursors with Positive and Unlabeled Machine Learning*, ACS  
30 Nano **13**, 3031, (2019).
- 31 [59] A. V. Smirnov, S. G. Ponomarev, V. P. Tarasovskii, V. V. Rybal'chenko, A. A. Vasin, and V. V. Belov, *Hard-*  
32 *Sphere Close-Packing Models: Possible Applications for Developing Promising Ceramic and Refractory Materials*,  
33 GLASS CERAM+ **75**, 345, (2019).
- 34 [60] C. J. Pickard and R. J. Needs, *Metallization of aluminum hydride at high pressures: A first-principles study*,  
35 Phys. Rev. B **76**, 144114, (2007).
- 36 [61] C. J. Pickard and R. J. Needs, *High-pressure phases of silane*, Phys. Rev. Lett. **97**, 045504 (2006).
- 37 [62] A. Shamp, T. Terpstra, T. Bi, Z. Falls, P. Avery, and E. Zurek, *Decomposition Products of Phosphine Under*  
38 *Pressure: PH<sub>2</sub> Stable and Superconducting?*, J. Am. Chem. Soc. **138**, 1884, (2016).
- 39 [63] D. Duan, X. Huang, F. Tian, D. Li, H. Yu, Y. Liu, Y. Ma, B. Liu, and T. Cui, *Pressure-induced decomposition of*  
40 *solid hydrogen sulfide*, Phys. Rev. B **91**, 180502(R), (2015).
- 41